

Adaptive Class Weight based Dual Focal Loss for Improved Semantic Segmentation

Md Sazzad Hossain, Andrew P. Paplinski, and John M. Betts

Faculty of Information Technology, Monash University, Melbourne, Australia.
sazzad.hossain, andrew.paplinski, john.betts@monash.edu

Abstract— In this paper, we propose a Dual Focal Loss (DFL) function, as a replacement for the standard cross entropy (CE) function to achieve a better treatment of the unbalanced classes in a dataset. Our DFL method is an improvement on the recently reported Focal Loss (FL) cross-entropy function, which proposes a scaling method that puts more weight on the examples that are difficult to classify over those that are easy. However, the scaling parameter of FL is empirically set, which is problem-dependent. In addition, like other CE variants, FL only focuses on the loss of true classes. Therefore, no loss feedback is gained from the false classes. Although focusing only on true examples increases probability on true classes and correspondingly reduces probability on false classes due to the nature of the softmax function, it does not achieve the best convergence due to avoidance of the loss on false classes. Our DFL method improves on the simple FL in two ways. Firstly, it takes the idea of FL to focus more on difficult examples than the easy ones, but evaluates loss on both true and negative classes with equal importance. Secondly, the scaling parameter of DFL has been made learnable so that it can tune itself by backpropagation rather than being dependent on manual tuning. In this way, our proposed DFL method offers an auto-tunable loss function that can reduce the class imbalance effect as well as put more focus on both true difficult examples and negative easy examples. Experimental results show that our proposed method provides better accuracy in every test run conducted over a variety of different network models and datasets.

Keywords—Deep neural network, semantic segmentation, cross entropy, class imbalance, focal loss

I. INTRODUCTION

Segmentation is a crucial part of image processing tasks. From medical imaging to autonomous vehicles, segmentation plays a key role to associate variety of image-based applications. Deep neural network-based semantic segmentation has recently gained popularity due to its high level of accuracy and computational efficiency [1]. A limitation of traditional approaches, such as intensity, edge or hand-crafted feature based segmentation is that accuracy tends to reduce in the presence of complex textures or when image quality is low. Semantic segmentation, however, overcomes these difficulties by breaking down the image into high-to-low level feature maps by using encoder-decoder type deep neural network (DNN) models and adapting them to the specifics of the data during training [2].

In addition, the availability of powerful computational resources and many publicly available datasets has made semantic segmentation increasingly popular and accessible to researchers over recent years [3]. Because semantic segmentation is a pixelwise classifier, it can suffer from class imbalance. That is, when the occurrence of each class is not evenly distributed in terms of pixel count, the network will be biased towards classes having the greatest number of examples, which degrades overall performance [4]. To address this issue, a popular technique is to apply a weight factor to the loss function so that the probabilistic decision is balanced between the classes. A number of studies dealing with class imbalanced datasets have reported that such weighting techniques can improve the classification accuracy, for example, [5, 6].

The ideal setting of class weight parameters is a challenge. In addition to determining the class weight parameters by trial and error [7-9], another common technique to set the weight factor by using the inverse of the number of pixels belonging to each class [5, 10-12]. Although trial and error may yield suitable weight values, it is troublesome as it involves manual adjustment over multiple test runs, which still would not guarantee an optimal classification result. On the other hand, such pixel frequency based method of setting weight parameters may not always reliably produce the most accurate semantic segmentation results, because semantic segmentation performance is more affected by spatial distribution and correlation of the pixels [13] rather than pixel frequency of individual classes alone. Therefore, it is necessary to find a way to identify "hard-to-classify" examples and assign greater weights to them. Focusing this idea, a recent variant of CE namely 'Focal Loss' introduces an effective weighting technique, which defines the class weight factor as a function of network's prediction confidence as shown in Sec III of this paper. In this way, hard examples would receive more loss than the easy examples to balance the overall loss. Although authors showed that FL outperforms conventional weighted cross entropy, its primary limitation like other CE variants is that it only evaluates the loss on true/positive classes. That is, it defines a hard example only by the low prediction score on true classes and elevates the weight factor accordingly. So, if high probability score is obtained on the negative classes, it assigns zero penalty to the network. So the network behaves blind on the negative classes. Although softmax function automatically

reduces the probability score on negative classes when probability on the positive class raises, the network does not train its parameters to produce lower probability on the negative classes. Hence, the network accuracy remains stuck in a ‘pseudo global minima’, which can be alleviated by considering the loss on the negative classes. Another limitation of FL, like all other variants of CE, is that it consists of a scaling coefficient, which is set empirically. So, it is likely that if this scaling coefficient can be optimized automatically depending on the loss function, it would further improve the class weighting effect. Considering these issues, we propose a novel Adaptive Class Weight based Dual Focal Loss (ADFL) technique, whereby the scaling coefficient is learnable and is optimized during the training of the network. This is achieved by introducing an additional layer prior to the softmax layer, which we refer to as the "Adaptive class weight (ACW) layer". The weighted cross entropy function is then replaced by the Dual Focal Loss (DFL) function in the classification layer. We show that ACW layer equivalently produces a scaling/weighting factor similar to that of FL and weighted cross entropy (WCE) influencing the softmax output, except it is trainable in our proposal.

The accuracy and consistency of our method is tested under varying conditions by performing semantic segmentation on three different datasets using three different fully convolutional network (FCN) models. The FCN models are: DeepLabV3+ [1], Ronneberger’s U-net [14] and VGG19 FCN [15]. The datasets used are: the MICCAI MRI datasets on prostate segmentation [16], transrectal (TRUS) ultrasound image datasets of prostate and Cityscape datasets [17]. Besides, as our proposed scaling coefficient is trainable, we also checked our method using two most popular training algorithms – adaptive moment estimation (ADAM) [18] and stochastic gradient descent with momentum (SGDM) [19] to investigate their effect on our method.

The later part of this paper discusses about some relevant works, describes the proposed methodology in details and analyses the results of different experimentations.

II. RELATED WORKS

Multiple strategies have been proposed in recent years to address the class imbalance problem. Although not all of them are centred on semantic segmentation, these approaches are interchangeable between any application domain that concerns class imbalance issue. The most common approach is to impose effective sampling methods. That is, these methods mainly focus on designing the datasets than operating on the DNN models. For instance, Havaei et al. [20] proposed a two-phase training technique to balance the class distribution. They first trained their DNN with a dataset containing equal number of labels so that the DNN learns the image features initially. Then they deployed a second training by keeping the weights fixed, but tuning only the output layer using a more representational set of datasets. A similar strategy was followed by Matthew [21] who evenly distributed the training samples with positive and negative examples. However, such data sampling methods would require a plentiful of dataset for the DNN to learn image features properly using a balanced subsample. Another approach is to replicate the data of minority classes, commonly known as ‘oversampling’ [22]. Although this method has been used in several studies [23-25] and proven to be marginally effective, it

can cause overfitting as depicted in [26, 27]. To avoid such overfitting, Jo and Japkowicz [28] divided the datasets into a number of clusters and then separately oversampled each cluster. Shen et al. [29] selectively chose the training examples to uniformly distribute the classes in each mini-batch. Guo and Viktor [30] produced synthetic datasets of hard examples of both majority and minority classes. So, oversampling methods essentially require extra preprocessing of dataset, which is troublesome when data volume is large. In contrast to oversampling, another approach is to ‘undersampling’ of majority classes, i.e. to remove the data belonging to majority classes in order to equal it to the minority classes. Although Drummond et al. [31] showed that undersampling is preferable to oversampling in some cases, it removes a part of data that would be rather useful to learn essential image features by the DNN.

A number of studies tackled the class imbalance issue by proposing modification to learning algorithms or training scheme. Thresholding is one of such methods, where the outputs are influenced by a threshold parameter. To set this threshold value, Lawrence et al. [32] used an optimization algorithm, whereas Richard and Lippmann [33] used a prior class probability based on class frequency. Another approach is to apply separate cost values to the classes. For instance, Kukar et al. [34] imposed a cost parameter to the learning rate so that examples with high cost affects more to weight updating. A similar widely popular approach is to apply a class weight parameter to the loss function itself [5, 10-12]. This approach mainly includes different variants of cross entropy (CE) loss function as CE is particularly effective on classification tasks [35]. For example, weighted cross entropy (WCE) [5, 36] is a very popular variant of CE, which applies a weighting factor to the standard CE loss. This weighting factor applies more loss to the minority classes and less to the majority classes. Hence, it tries to balance the loss between imbalanced classes. Li et al. [35] proposed a dual cross entropy (DCE) method, which combines standard CE with a different weighted CE version in order to increase the overall loss when prediction tends to shift to a false class. Lin et al. [6] proposed a CE variant namely Focal Loss (FL) where the weighting factor has been formulated as a function of output probability so that the hard examples will be given more priority than the easy examples. FL has been proven to be a better CE variant than WCE as it can reduce the class imbalance effect by assigning more loss to the weak-exampled classes. Although these CE variants has been proven to alleviate the class imbalance issue to some extents, they do not receive any loss feedback on negative/false classes preventing the network achieve the best performance. DCE technique [35] is an exception in this case, because it calculates loss on negative classes as well. However, based on its formulation, it produces more loss when probability on negative class is low and less loss when probability is high. This produces an opposite loss effect on the negative examples, although it considers negative examples unlike other CE variants. Apart from this, the evaluation of the associated weighting factors is done either based on pixel frequency of the classes or by trial and error. These procedures struggle to establish an optimal weight factor as classification accuracy depends more on spatial correlation between pixels than the number of examples per class [13]. Therefore, automatic optimization of the weight factor would

facilitate the learning process as well as the accuracy. Hence, this study was motivated to propose a novel loss function that would penalize the network on both positive and negative examples, produce more loss for hard examples and can be automatically scaled through backpropagation.

III. METHODOLOGY

A. Cross Entropy Loss

Cross entropy loss or log loss basically evaluates the classification performance of a classifier model. The intuition behind cross entropy loss is that a wrong probability distribution, \hat{P} will always require more bits of information which can be expressed as a negative logarithm of \hat{P} (Equation. (1)). Integrating this with the formula of expected/average probability of an event (Equation. ()), we get the expression of ‘entropy’ (Equation. (2)) that defines the expected value of an information having i possible cases.

$$\text{Information required, } I = -\log \hat{P} \quad (1)$$

$$\text{Entropy, } E(I) = -\sum_i \hat{P}_i \log \hat{P}_i, \quad (2)$$

However, entropy cannot measure how much deviated a distribution, \hat{P} is from the original/true distribution, P . Hence, ‘cross entropy’ was derived by adding KL divergence [37] as a distance measure between \hat{P} and P to the entropy function resulting in the expression of Equation. (3). This enables a classifier to quantify the deviation of its predicted probability, \hat{P} from the original probability, P over every class i .

$$\text{Cross entropy, } CE = -\sum_i P_i \log \hat{P}_i \quad (3)$$

B. Weighted Cross Entropy Loss

When a dataset contains imbalanced ratio of classes, the classifier tends to focus more on the class that has the most number of samples. This biases the classification performance to that particular class. Such class imbalance is very frequent in semantic segmentation problems where the number of pixels per class varies differently. To address this, a popular practice is to use weighted cross entropy (WCE) loss function. WCE is a variant of standard CE with an additional ‘class weight’ parameter, w_i as the following equation:

$$WCE = -\sum_i w_i P_i \log \hat{P}_i \quad (4)$$

w_i is inversely related to the number of pixels under class i . In this study, we used the inversed normalized pixel frequency of the classes as given in Equation. (5),

$$w_i = \frac{|X|/|X_i|}{\sum_i (|X|/|X_i|)} \quad (5)$$

where, X and X_i indicates the entire pixel set and the pixel set belonging to class i from the training images respectively.

In this way, the loss function acts more sensitive to the minority classes and less sensitive to the majority ones.

C. Focal loss

Focal loss (FL) is a recent variant of WCE. The key feature of FL is that it formulates the weighting factor as a function of prediction confidence of the DNN as shown in Equation (6). In doing so, the classes with low prediction accuracy, i.e. hard examples would receive higher loss than the easy examples.

$$FL = -\sum_i \alpha_i (1 - \hat{P}_i)^\gamma \log \hat{P}_i \quad (6)$$

Equation (6) shows that FL has two additional scaling coefficients $-\alpha$ and γ to control the degree of weighting. When $\gamma = 0$, FL becomes the WCE and α acts as the class weight parameter. When $\gamma \geq 1$, the weighting factor $(1 - \hat{P}_i)^\gamma$ increases with decreasing \hat{P}_i and vice-versa. Therefore, when \hat{P}_i of a particular class is lower, the weighting factor becomes larger and hence the loss value on that class. To avoid the weighting factor to be larger than necessary, scaling coefficient $-\alpha$ is applied to diminish the weight intensity. The original paper showed that $\gamma = 2$ and $\alpha = 0.25$ yields the best performance.

D. Dual focal loss

For both binary and multi-class classification problem, softmax is the most commonly used function to evaluate the probabilistic output. Softmax converts its input into a one-hot vector, i.e. a vector containing probability score of each class ranging (0, 1). Then CE calculates the loss using the ground truth probability $P_i \in \{0, 1\}$ as shown in Equation 3. So, the standard CE only takes the loss on positive classes when $P_i = 1$. For negative classes, CE becomes 0 as $P_i = 0$. As a result, the CE function simply becomes a negative logarithm of \hat{P}_i . Therefore, for positive classes ($P_i = 1$), when $\hat{P}_i \rightarrow 1$, $CE \rightarrow 0$. However, for negative classes ($P_i = 0$), CE becomes 0 even if $\hat{P}_i \rightarrow 1$. It means that the loss becomes zero even if the predicted output gained high confidence on false classes. So, when WCE or FL is used, the weight is applied only to the predicted score on positive classes. This is problematic for the network to achieve proper learning. It is because during the training phase, particularly at initial stage, networks may often produce high \hat{P}_i score on false classes. When this occurs, CE, WCE and FL assign zero loss to the network and thus sends no feedback to the learning parameters causing the false high score of \hat{P}_i . Due to the same reason, although FL proved to be better than CE and WCE to address both class imbalance and class weakness, it increases the weight factor on ‘positive hard’ classes $\{\hat{P}_i: P_i = 1, \hat{P}_i \ll 1\}$ only and remains blind to the ‘negative easy’ $\{\hat{P}_i: P_i = 0, \hat{P}_i \rightarrow 1\}$ classes.

To address this issue, we propose a new CE variant named Dual Focal Loss (DFL), which takes into account the loss on false classes as well in addition to the loss on true classes. Besides, it produces a similar weight factor to that of FL, which focuses more on hard examples by using the squared difference between the ground truth P_i and the predicted output \hat{P}_i as shown in Equation (7).

$$DFL = -\sum_i \log(1 - (P_i - \hat{P}_i)^2) \quad (7)$$

The visualization of the DFL, FL and CE has been shown in Figure 1. It can be seen that DFL produces similar curve to FL when $P_i = 1$. However, when $P_i = 0$, FL is zero for all \hat{P}_i , whereas DFL produces more loss on high \hat{P}_i and less loss on low \hat{P}_i score. Therefore, unlike FL, DFL can produce weighted loss on both positive and negative classes, which increases logarithmically as $(P_i - \hat{P}_i)^2$ increases. In doing so, the network will achieve better learning by simultaneously reducing loss on both true and false classes.

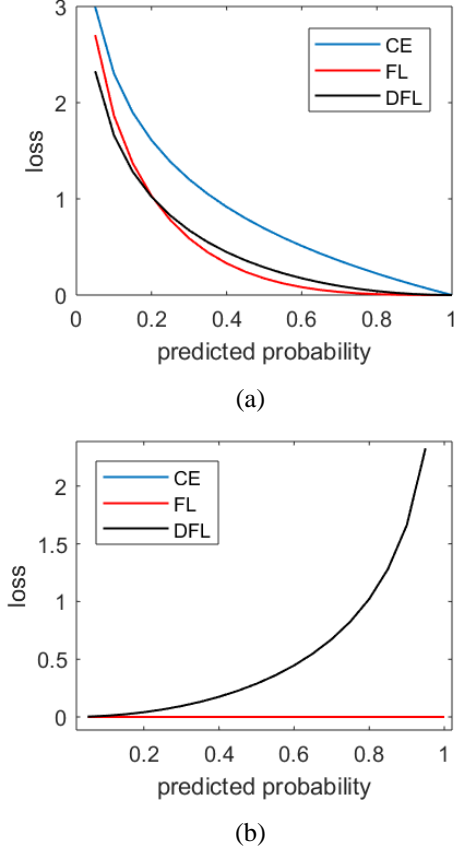


Fig. 1. Loss vs. predicted probability for CE, FL and DFL when (a) ground truth probability = 1 and (b) ground truth probability = 0

Now, instead of softmax, if sigmoid function is used when dealing with a binary classification problem, the loss is also evaluated on negative classes as well. In this case, CE and FL are expressed as Equation. Another recent CE variant DCE, as expressed in Equation, also produces loss on negative classes and claims to be applicable to both binary and multi-class classification problem.

$$CE = -P_i \log(\hat{P}_i) - (1 - P_i) \log(1 - \hat{P}_i) \quad (8)$$

$$FL = -\alpha(1 - \hat{P}_i)^\gamma P_i \log(\hat{P}_i) - (1 - \alpha)(1 - \hat{P}_i)^\gamma (1 - P_i) \log(1 - \hat{P}_i) \quad (9)$$

$$DCE = -P_i \log(\hat{P}_i) + \beta(1 - P_i) \log(\alpha + \hat{P}_i) \quad (10)$$

(where, $\beta, \alpha > 1$)

So, the derivative of CE, FL and DCE with respect to \hat{P}_i can be expressed as,

$$\frac{\partial}{\partial \hat{P}_i}(CE) = -\frac{P_i}{\hat{P}_i} + \frac{1 - P_i}{1 - \hat{P}_i} \quad (11)$$

$$\begin{aligned} \frac{\partial}{\partial \hat{P}_i}(FL) = & -\frac{\alpha(1 - \hat{P}_i)^\gamma P_i}{\hat{P}_i} \\ & + \alpha\gamma(1 - \hat{P}_i)^{\gamma-1} P_i \log(\hat{P}_i) \\ & + \frac{(1 - \alpha)(1 - \hat{P}_i)^\gamma (1 - P_i)}{1 - \hat{P}_i} \\ & - (1 - \alpha)\gamma(1 - \hat{P}_i)^{\gamma-1} (1 - P_i) \log(1 - \hat{P}_i) \end{aligned} \quad (12)$$

$$\frac{\partial}{\partial \hat{P}_i}(DCE) = -\frac{P_i}{\hat{P}_i} + \beta \frac{1 - P_i}{\alpha + \hat{P}_i} \quad (13)$$

Equation (11)-(13) shows that in the best case scenario, i.e. when $P_i = \hat{P}_i = 1$ or 0 , $\frac{\partial}{\partial \hat{P}_i}(CE) = 1$, $\frac{\partial}{\partial \hat{P}_i}(FL) > 0$ (since $\alpha, \gamma > 0$) and $\frac{\partial}{\partial \hat{P}_i}(DCE) > 0$. Therefore, the derivative of CE, FL and DCE never becomes zero even when the prediction equals to the ground truth probability. It means that even upon achieving the best result, the network still tries to update its learnable parameters since the derivative of loss never becomes zero. In addition, for a greater value of \hat{P}_i when $P_i = 0$, the training becomes instable as $\frac{\partial}{\partial \hat{P}_i}(FL)$ produces lower loss for false high value of \hat{P}_i . This is why the original study used a bias term π , which forces the sigmoid function to produce a lower value of \hat{P}_i on negative classes, which in turn provides a wrong or nearly zero feedback to the network as to why negative classes gained high probability score.

On the other hand, the derivative of DFL is,

$$\frac{\partial}{\partial \hat{P}_i}(DFL) = -\frac{2(P_i - P_i)}{1 - (P_i - \hat{P}_i)^2} \quad (14)$$

So, Equation 14 shows that when $P_i = \hat{P}_i = 1$ or 0 , $\frac{\partial}{\partial \hat{P}_i}(DFL) = 0$. Therefore, when prediction matches to the ground truth, DFL produces no further loss and hence the network stops updating its learnable parameters. Besides, since $\log(0) = \infty$, \hat{P}_i always needs to be bounded away from zero for all other CE variants, which is not necessary when using DFL.

In Equation 7 noticeable that the other scaling coefficient $-\alpha$, used in FL, is absent in DFL. It is because we propose to make this parameter learnable by backpropagation so that it can tune itself to an optimal value depending on the training dataset. Besides, unlike FL, we designed α as a class-wise parameter, i.e. to be individual for each class to induce an additional class-balancing effect. The following section explains our proposed technique to make α parameter learnable.

E. Adaptive class weight layer

The scaling coefficient α used in FL is equivalent to the class weight parameter w_i used in WCE. While α in FL was set empirically in the original paper, w_i in WCE is usually set either empirically or by using inverse pixel frequency. However, the biasness of DNN models may not always be proportional to the number of samples per class which produces the value of w_i . For example, in semantic segmentation tasks, if the region of interest in the image is noisy, the output might be erroneous even if that region of interest belongs to the majority class. Therefore, the optimal value of w_i is unlikely to be achieved using the number of pixels per class. To this end, we propose a scheme where the class weight parameter, or equivalent scaling coefficient for DFL, will be adaptively adjusted during the training phase. For this, we simply multiply the input x of the softmax layer by an adaptive class weight parameter \widehat{w}_i . The following part shows how this scheme equivalently produces similar loss effect to standard WCE.

For any class i , the output of the softmax layer (S_i), which is the previous layer of the cross entropy loss layer, is given by,

$$S_i = \frac{e^{x_i}}{\sum_{i=1}^n e^{x_i}} \quad (15)$$

where, x is the input to the softmax layer; n is the number of classes.

Since S_i is the input to the cross entropy loss layer, Equation. (4) becomes,

$$WCE = -w_i P_i \log\left(\frac{e^{x_i}}{\sum_{i=1}^n e^{x_i}}\right) \quad (16)$$

As $P_i \in \{0, 1\}$, CE and WCE is only active when $P_i = 1$. Therefore,

$$\begin{aligned} WCE &= -w_i \left(\log(e^{x_i}) - \log\left(\sum_{i=1}^n e^{x_i}\right) \right) \\ \Rightarrow WCE &= -w_i \left(x_i - \log\left(\sum_{i=1}^n e^{x_i}\right) \right) \end{aligned} \quad (17)$$

Now, when we multiply the softmax layer input x by w_i , the output of the softmax layer becomes,

$$S_i = \frac{e^{w_i x_i}}{\sum_{i=1}^n e^{w_i x_i}} \quad (18)$$

Using Equation (18), the standard CE loss shown in Equation (3) becomes:

$$CE = -\log\left(\frac{e^{w_i x_i}}{\sum_{i=1}^n e^{w_i x_i}}\right) \quad (19)$$

$$\Rightarrow CE = -\left(w_i x_i - \log\left(\sum_{i=1}^n e^{w_i x_i}\right) \right) \quad (20)$$

Subtracting Equation. (20) from Equation. (17),

$$\begin{aligned} WCE - CE &= \left(-w_i x_i + w_i \log\left(\sum_{i=1}^n e^{x_i}\right) \right) \\ &\quad - \left(-w_i x_i + \log\left(\sum_{i=1}^n e^{w_i x_i}\right) \right) \\ &= -w_i x_i + w_i \log\left(\sum_{i=1}^n e^{x_i}\right) + w_i x_i - \log\left(\sum_{i=1}^n e^{w_i x_i}\right) \\ &= w_i \log\left(\sum_{i=1}^n e^{x_i}\right) - \log\left(\sum_{i=1}^n e^{w_i x_i}\right) \\ &= \left(\log\left(\sum_{i=1}^n e^{x_i}\right)^{w_i} - \log\left(\sum_{i=1}^n e^{w_i x_i}\right) \right) \\ &= \log\left(\frac{\left(\sum_{i=1}^n e^{x_i}\right)^{w_i}}{\left(\sum_{i=1}^n e^{w_i x_i}\right)}\right) \\ &= \text{constant for any class } i \end{aligned}$$

**\therefore Adaptive class weight with standard cross entropy
= Weighted cross entropy – constant**

Therefore, we can see that if we multiply the same weight w_i with the softmax layer's input x and pass the output to non-weighted cross entropy layer, the resultant output will be equivalent to the output of the weighted cross entropy layer with only difference of a constant. So, the derivative of both weighted cross entropy and adaptive class-weighted cross entropy remains unchanged, but adaptive class weight provides the opportunity to tune the class weight parameter automatically.

Based on this idea of weighting the softmax input, we use an adaptive class weight (ACW) layer for DFL, which would provide additional scaling effect similar to α in FL. Now, instead of using ACW layer, if we use a fixed scaling coefficient α like FL, $\alpha > 1$ would enlarge the loss and $\alpha < 1$ would decrease it. Due to this, if DFL produces a higher loss on a particular class, $\alpha < 1$ would reduce it and thus prevent the network to put more focus on that class. In contrast, if DFL produces a lower loss, $\alpha > 1$ would make the network focus more on that class, which may lead to overfitting and under-focusing on the weak classes. Hence, as stated earlier, choosing the proper α value manually is challenging as it requires plenty of test runs, which is time-consuming and troublesome. This is why instead of using a fixed scaling coefficient like α in FL or w_i in WCE, a flexible weight factor \widehat{w}_i , which can be obtained by ACW layer, should be used so that it can tune itself appropriately based on the loss feedback from DFL.

Thereby, we inserted an extra layer named "Adaptive class weight" (ACW) layer (Figure 2) in order of automatic tuning of \widehat{w}_i to facilitate DFL.

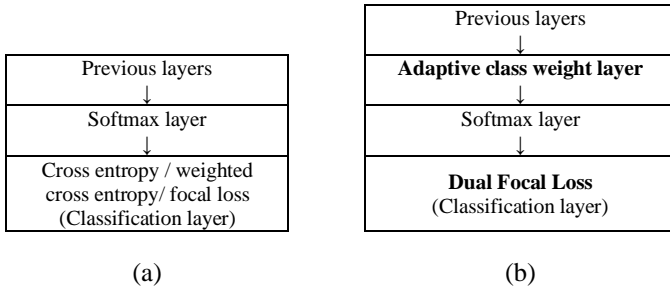


Fig. 2. (a) Standard DNN model (b) Proposed modification to DNN model

Therefore, for any input x_i , the output of the ACW layer Z_i on any class i becomes,

$$Z_i = \widehat{w}_i x_i \quad (21)$$

Hence, our proposed methodology can be summarized as follows:

- A new loss function – DFL has been proposed, which follows the idea of FL to impose more loss on hard examples and less on easy examples. However, unlike FL or any of the state-of-the-art CE variants, DFL can impose loss on both positive and negative classes, and it can impose more loss on false high probability score. So, at the same time, DFL can focus on ‘true hard’ ($\{\widehat{P}_i: P_i = 1, \widehat{P}_i \ll 1\}$) examples as well as ‘false easy’ ($\{\widehat{P}_i: P_i = 0, \widehat{P}_i \rightarrow 1\}$) examples.
- A new layer (ACW) is inserted before the softmax layer which offers a tuneable scaling coefficient to DFL in order to influence the intensity of loss automatically.

Since the proposed method is the combination of ACW layer and DFL, we name it as ‘ADFL’ and use this acronym in the later part of this paper.

IV. EXPERIMENTATION SCHEME

A. DNN models and datasets

Semantic segmentation tasks require fully a different variant of DNN known as fully convolutional networks (FCNs). FCN basically replaces the fully connected layer of a DNN with convolution and upsampling layers, which produces a pixelwise classification output of an image. In this study, we used three different DNN models – DeepLabV3+ [1], VGG19 FCN [2, 15] and Ronneberger’s U-net [14] in order to ensure the effectiveness of the proposed scheme over different cases. For DeepLabV3+, we used ResNet-18 [38] as the backbone architecture. The structural details and description of each of the FCNs are provided in the corresponding cited references.

Three different datasets have been used here, which are – 1) MICCAI MRI datasets of prostate 2) Transrectal Ultrasound (TRUS) images of prostate, and 3) Cityscape datasets. Due to availability and usage in some of our previous studies, we used the MRI and TRUS datasets of prostate here. Although PASCAL VOC2012 [39] and COCO [40] are also two popularly used datasets, we did not use them in our experiment due to limitation of computational resources to train the FCNs on such large datasets. Instead, we took Cityscape [17] as our third

dataset which contains relatively smaller number of images. This dataset contains total 701 images of a city’s street view with total 11 classes, which are: *sky, cars, buildings, trees, fence, pedestrians, bicyclists, road, pavement* and *signpost*. The MRI datasets are a part of MICCAI Grand Challenge Datasets 2012 [16], which contains 3D MHD formatted images of prostate from total 80 patients. This dataset consists of only two classes – *prostate* region and *background* region. The TRUS datasets were collected from Alfred Hospital, Melbourne, which consists of 3D DICOM formatted volumetric ultrasound images of prostate of 5 patients. Like MRI, TRUS dataset also contains two classes only - *prostate* and *background* region. These TRUS images were obtained through proper ethical clearance from both Alfred hospital and Monash University. Some visual examples of all three datasets have been shown in Figure 3. Since we will perform semantic segmentation on 2D images only, we broke down all volumetric images into sets of 2D images. Each of the images were resized into 224x224 dimension to match the default input image size of the FCN models. Both MRI and TRUS images are single-channelled as they are grayscale images, whereas Cityscape images are of three channels for being RGB images. All images were in portable network graphics (PNG) format to avoid compression loss as well as obtain the original quality of the image. The total size of each datasets and their distribution into training and testing sets have been given in Table 1.

Table 1. Size and distribution of datasets

Datasets	Total size	Training size	Testing size
MICCAI MRI of prostate	1378	1309	69
TRUS prostate	55	47	8
Cityscape	701	665	36

A. Platform and computational resource

We used MATLAB throughout the experiment including building the FCN models, conversion of 3D volumetric images into 2D image sets, training and testing the models with the datasets. To accelerate the computational time, we used MASSIVE High Performance Computing (HPC) which is a computer cluster provided by Monash University. This computing unit was configured with 13 processors, 120GB of Memory and Nvidia Tesla K80 GPU. For training algorithm, we used two most popular methods – SGDM [19] and ADAM [18]. This will reveal how training algorithms would affect the proposed ACE since it involves a learnable parameter. As the training parameters, we used initial learning rate – 0.0005, momentum – 0.9, mini-batch size – 4, learn rate drop factor – 0.95 and learn rate drop frequency – 5. These parameters were kept constant for all FCN models and datasets. However, the number of epochs varied for different FCN models and datasets, which was set using a small portion of the testing set as the validation set. To have a fair comparison between the loss functions, we used the same number of epochs for a given FCN model and dataset. In addition, we controlled the weight initialization so that weights are always initialized with the same values. In doing so, we subdue the effect of epoch number and random weight initialization on networks’ outcome.

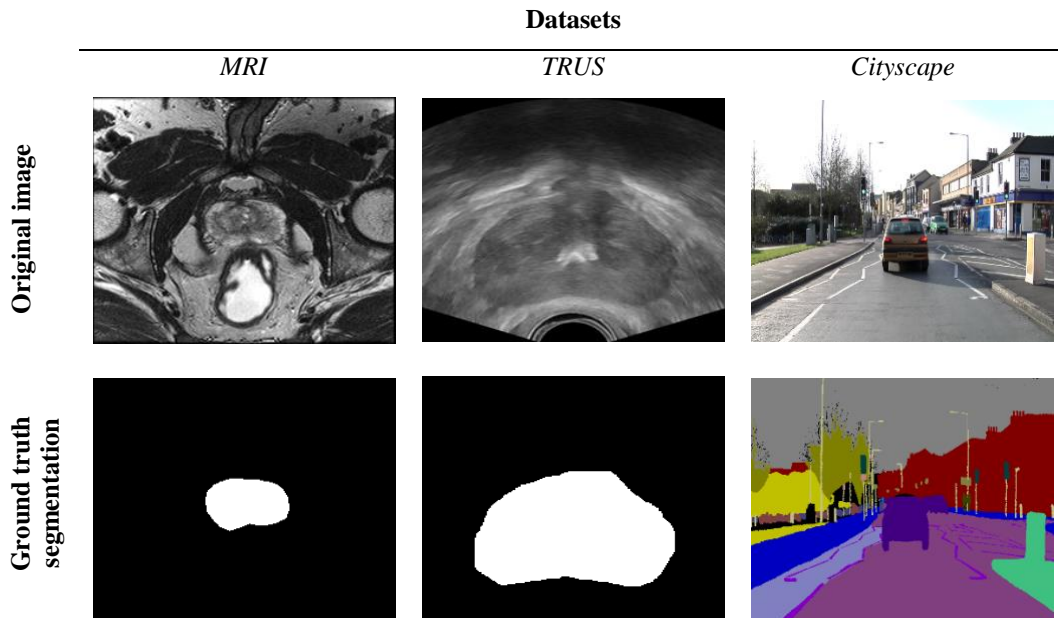


Fig. 3. Example images of the datasets with their ground truth labels

B. Metrics

We used two common metrics: Dice Similarity Coefficient (DSC) and mean Intersection over Union (mIOU) to quantify the segmentation accuracy. Mathematically, they are expressed as follow:

$$DSC = 2 \frac{|X \cap Y|}{|X| + |Y|} \quad (15)$$

$$IOU = \frac{|X \cap Y|}{|X| + |Y| - |X \cap Y|} \quad (16)$$

where, X and Y are number of pixels belonging to "ground truth" and "predicted" region of a particular class. The modulus sign ' $|$ ' indicates the cardinality of the respective sets.

To quantify the overall accuracy of each test run, we calculated the mean DSC (mDSC) and mean IOU (mIOU) of the predicted segmentation on the test images. For MRI and TRUS datasets, mDSC and mIOU were measured for the 'prostate' region only. It is because 'background' region is much larger than the 'prostate' region and so network's segmentation on 'background' region would naturally be of greater accuracy, which would falsely increase the overall accuracy.

V. RESULTS AND DISCUSSION

A. Performance of ADFL across different conditions

The overall experiment of this study consists of three sub-experiments, where each one tests the consistency of performance of ADFL by varying a particular condition such as

FCN models, training algorithms and datasets. In all sub-experiments, ADFL was compared with standard CE and WCE on different conditions. Besides, each sub-experiment was conducted with three test runs repeated three times to ensure the consistency of the outcome. Each test run was done with different set of test data, which resembles to 3-fold cross-validation. In all other sub-experiments except 2 (where the proposed method was tested on different datasets) only TRUS dataset was used, because these sub-experiments comprise a large number of total test runs, where TRUS dataset would quicken each test due to having the smallest number of images.

Our first sub-experiment tests the performance of ADFL when different FCN models are used as shown in Table 2. In this case, the training algorithm and dataset were ADAM and TRUS respectively, which were kept fixed for this sub-experiment.

Table 2 shows that ADFL resulted in the best accuracy with every FCN model at every test run. After ADFL, FL found to be the 2nd best across all FCN models, although in few cases (such as with VGG19 FCN) FL was outperformed by CE and/or WCE. It is also noticeable that although WCE is better than CE in majority of the cases, WCE does not always produce better accuracy than CE, such as when VGG19 FCN was used. This indicates that balanced loss distribution is not always guaranteed with WCE loss function. Model-wise, DeepLabV3+ provides the best accuracy for all loss functions, while U-net the least.

Our second sub-experiment tests ADFL over different datasets as shown in Table 3. For this sub-experiment, DeepLabV3+ has been used as the FCN model and ADAM as the training algorithm. Table shows that ADFL always yields the best accuracy for each of the datasets.

Table 2. Performance comparison of ADFL over different FCN models.

Conditions (Loss function + FCN models)	Test run#1		Test run#2		Test run#3	
	mDSC (%)	mIOU (%)	mDSC (%)	mIOU (%)	mDSC (%)	mIOU (%)
WCE+DeepLabV3+	84.45	74.57	83.10	71.81	83.88	73.26
CE+DeepLabV3+	82.43	71.81	80.75	69.82	83.22	73.29
ADFL+ DeepLabV3+	89.23	81.62	86.42	78.46	85.75	77.41
FL+DeepLabV3+	85.52	77.59	83.43	73.08	84.24	73.74
WCE+VGG19 FCN	79.29	68.57	73.71	62.55	78.28	68.92
CE+VGG19 FCN	77.90	65.81	73.85	63.00	78.73	68.82
ADFL+VGG19 FCN	79.90	69.01	79.94	68.23	80.18	69.64
FL+VGG19 FCN	76.40	64.31	77.94	65.17	77.13	65.09
WCE+U-net	62.69	46.10	75.13	60.50	58.50	41.97
CE+U-net	60.13	47.00	70.03	57.84	66.38	56.42
ADFL+U-net	79.18	70.81	78.73	63.24	78.80	67.58

Table 3. Performance comparison of ADFL over different datasets.

Conditions (Loss function + datasets)	Test run#1		Test run#2		Test run#3	
	mDSC (%)	mIOU (%)	mDSC (%)	mIOU (%)	mDSC (%)	mIOU (%)
WCE+MRI	81.89	71.24	82.52	72.05	81.74	71.23
CE+MRI	83.63	77.93	83.17	78.04	82.20	75.35
ADFL+MRI	89.49	83.54	89.51	83.59	87.50	81.90
FL+MRI	84.78	75.26	84.12	74.88	85.28	75.12
WCE+TRUS	81.68	71.17	83.92	74.47	82.12	72.47
CE+TRUS	82.14	72.15	84.36	76.08	82.71	72.56
ADFL+TRUS	86.90	77.37	86.09	77.16	85.89	75.93
FL+TRUS	84.21	74.82	76.50	64.59	84.09	75.72
WCE+Cityscape	63.26	54.22	66.63	57.86	66.01	57.87
CE+Cityscape	60.91	53.09	65.35	57.24	65.79	57.82
ADFL +Cityscape	68.43	60.31	67.24	59.01	66.92	59.05
FL+Cityscape	68.31	60.38	64.08	56.74	65.44	58.16

Table 3 shows that ADFL produced the best accuracy among CE, WCE and FL for every dataset. Besides, like the 1st sub-experiment, FL is the 2nd best in this sub-experiment as well, although it produced lesser accuracy than CE and WCE in few cases. While ADFL causes slight accuracy improvement on Cityscape dataset, it substantially elevates the accuracy on MRI and TRUS datasets. Between CE and WCE, CE seemed to produce better accuracy than WCE on MRI and TRUS datasets in every test run, whereas WCE performed better on Cityscape dataset. This depicts that WCE does not always outperform CE on any dataset, but with more appropriate weight factor obtained from DFL or FL, the accuracy can definitely be improved than CE and WCE.

As the third and final sub-experiment, we test ADFL for two different training algorithms: ADAM and SGDM. The main purpose of this sub-experiment is to check the effect of training algorithm on our proposed ACE since it contains a learnable parameter. In this case, we used DeepLabV3+ with TRUS datasets for all cases.

Results in Table 4 shows that ADFL produces the best accuracy for both ADAM and SGDM among WCE, CE and FL. The accuracy level obtained from ADAM is much higher than that from SGDM for every loss function in every cases. For both ADAM and SGDM, it is noticeable that WCE produces the best accuracy following DFL in almost every test run, whereas FL was the 2nd best in the previous two sub-experiments. CE always produced the least accuracy except with ADAM at test run#1.

Table 4. Performance comparison of ADFL over different training algorithms.

Conditions (Loss function + training algorithm)	Test run#1		Test run#2		Test run#3	
	DSC (%)	mIOU (%)	DSC (%)	mIOU (%)	DSC (%)	mIOU (%)
WCE+ADAM	84.72	75.00	85.13	76.01	84.95	75.55
CE+ADAM	81.18	70.94	79.64	70.74	71.78	62.70
ADFL+ ADAM	87.58	79.13	87.41	78.76	88.54	80.16
FL+ADAM	84.61	74.62	84.81	75.66	86.95	78.70
WCE+SGDM	69.94	55.30	69.73	55.39	68.99	54.11
CE+SGDM	54.80	41.77	58.78	45.39	58.98	46.14
ADFL+SGDM	75.56	63.42	74.59	61.97	75.61	63.43
FL+SGDM	62.82	50.04	63.09	50.15	63.46	50.35

Therefore, the above results prove that ADFL can outperform the present CE function based loss functions such as standard CE, WCE and FL for any data, FCN model and training algorithm. Although different dataset, FCN model or training algorithm may produce different accuracy level, the relative accuracy of ADFL will always be higher than that of CE, WCE and FL.

B. Mutual dependency of ACW layer and DFL

The purpose of the scaling parameter α of both FL and DFL is to interact with the γ parameter in order to induce further accuracy. The study of FL showed that with a suitable α value, FL yields more accuracy than without α . Since α is automatically evaluated with backpropagation in this study, it is important to check how it influences the proposed loss function – DFL, or in other word, the mutual dependency of ACW layer and DFL. To do this, we checked the accuracy for DFL without ACW layer, ACW layer without DFL and for combined DFL and ACW layer (i.e. ADFL) on all three datasets using DeepLabV3+ and ADAM as shown in Table 5.

Table 5. Importance of the combination of ACW layer and DFL

Conditions	mDSC (%)	mIOU (%)
DFL without ACW layer + MRI	90.74	84.68
DFL with ACW layer + MRI	90.98	85.52
ACW layer without DFL + MRI	86.30	78.50
DFL without ACW layer + TRUS	83.39	76.77
DFL with ACW layer + TRUS	87.14	77.75
ACW layer without DFL + TRUS	86.56	77.50
DFL without ACW layer + Cityscape	65.15	57.96
DFL with ACW layer + Cityscape	67.84	59.86
ACW layer without DFL + Cityscape	64.27	55.02

Table 5 shows that when only DFL is used without the ACW layer, which contains the adaptive scaling parameter, the accuracy degrades to different extents for different datasets. When only the ACW layer is used with standard CE, i.e. without DFL, it degrades the accuracy as well. Therefore, both ACW layer and DFL are needed to be used in combination in order to obtain the highest accuracy than using just either of them. The reason is that while DFL makes the loss function puts more focus on hard examples of both positive and negative classes, ACW layers fine-tune the loss to improve the accuracy.

C. Importance of ACW layer over WCE

As discussed in Sec III, the adaptive weight factor α in the ACW layer with standard CE as the loss function works equivalently as the weight factor used in WCE. Comparing Table 3 and 5, we can see that ACW layer produces better accuracy than WCE when CE is used as the loss function. It means that ACW layers produces a better weight factor than the weight factor used in WCE. To confirm this, we compared WCE with ACW layer-influenced CE using all three datasets with DeepLabV3+ and ADAM as shown in Table 6. This would reveal how ACW would perform solely with standard CE loss in place of WCE.

Table 6 shows that with standard CE and ACW layer, the network produces better accuracy than that with WCE, i.e. CE with conventional pixel frequency based class weight. Therefore, the ACW layer produces a better weight factor than w_i by automatic tuning through backpropagation and thus reduces the effort of manual tuning.

Table 6. Robustness of ACW layer based CE over WCE.

Conditions	mDSC (%)	mIOU (%)
ACW layer + CE + MRI	86.30	78.50
WCE + MRI	77.73	66.76
ACW layer + CE + TRUS	86.56	77.50
WCE + TRUS	84.62	74.28
ACW layer + CE + Cityscape	65.70	57.45
WCE + Cityscape	62.65	53.45

D. Robustness of DFL over FL

Comparing Table 3 and 5, it is visible that DFL without ACW layer produces better accuracy than FL. It means the proposed loss function – DFL enhances the idea of focusing on hard examples than FL. The reason, as discussed in Sec. III, is that while FL considers loss only on positive classes, DFL considers loss on both positive and negative classes, which enhances the training performance of the network. To confirm this, an additional experiment has been performed as shown in Table 7 where DFL was compared with FL without ACW layer using all three datasets with DeepLabV3+ and ADAM. To diminish the influence of α in FL, we use $\alpha = 1$.

Table 7. Robustness of DFL over FL.

Conditions	mDSC (%)	mIOU (%)
DFL + MRI	90.91	85.24
FL + MRI	89.16	83.88
DFL + TRUS	83.39	76.77
FL + TRUS	81.23	72.24
DFL + Cityscape	65.15	57.96
FL + Cityscape	63.92	54.47

Table 7 shows that DFL produces higher accuracy than FL in every case and hence proves that DFL acts as a better focal loss function than the original FL.

VI. CONCLUSION

In this paper, we propose an Adaptive Class Weight based Dual Focal Loss (DFL) technique to address the class imbalance and class weakness problems of semantic segmentation. This study was primarily motivated by the idea of Focal Loss (FL)

proposed by the Facebook AI research team. Unlike FL, our proposed DFL evaluates loss on both positive and negative classes as well as increasing the weight of hard-to-classify classes over those that are easy to classify. We have made the scaling coefficient in DFL learnable, thereby overcoming the limitations of previous approaches in which this parameter was set by trial and error or using inverse pixel frequency, neither of which could guarantee optimality. This parameter is tuned during the training phase by an "Adaptive class weight" (ACW) layer before the softmax layer. The performance of our new loss function was investigated on various network models, datasets and training algorithms. The experimental results are summarized below:

- The combination of DFL and ACW layer yields the highest semantic segmentation accuracy followed by FL in case of every dataset, training algorithms and FCN models.
- WCE does not always produce the best accuracy than CE depending on the datasets and FCN models. So, pixel frequency based class weight does not guarantee the best outcome.
- Using either DFL or ACW, rather than using together, results in slight decrease in accuracy. So, DFL and ACW layer should be used in combination to achieve the best outcome.
- ACW layer with standard CE yields better accuracy than WCE. So ACW layer produces better class weight effect than WCE.
- The proposed loss function – DFL outperforms the state-of-the-art CE variants.

Therefore, we have shown that our proposed loss function offers greater accuracy than FL and other loss functions by effectively addressing the class imbalance and class weakness issue in semantic segmentation using a novel formulation and scaling technique.

ACKNOWLEDGMENTS

The TRUS dataset was provided by the Alfred Hospital, Melbourne, and used subject to the relevant ethics approval of both Monash University and the Alfred Hospital. Computation was performed on the Massive™ HPC, Monash University.

REFERENCES

- [1] L.-C. Chen, Y. Zhu, G. Papandreou, F. Schroff, and H. Adam, "Encoder-decoder with atrous separable convolution for semantic image segmentation," in *Proceedings of the European conference on computer vision (ECCV)*, 2018, pp. 801-818.
- [2] J. Long, E. Shelhamer, and T. Darrell, "Fully convolutional networks for semantic segmentation," in *Proceedings of the IEEE conference on computer vision and pattern recognition*, 2015, pp. 3431-3440.
- [3] A. Paszke, A. Chaurasia, S. Kim, and E. Culurciello, "Enet: A deep neural network architecture for real-time semantic segmentation," *arXiv preprint arXiv:1606.02147*, 2016.
- [4] N. Japkowicz and S. Stephen, "The class imbalance problem: A systematic study," *Intelligent data analysis*, vol. 6, no. 5, pp. 429-449, 2002.

- [5] S. Xie and Z. Tu, "Holistically-nested edge detection," in *Proceedings of the IEEE international conference on computer vision*, 2015, pp. 1395-1403.
- [6] T.-Y. Lin, P. Goyal, R. Girshick, K. He, and P. Dollár, "Focal loss for dense object detection," in *Proceedings of the IEEE international conference on computer vision*, 2017, pp. 2980-2988.
- [7] J. Zhang, X. Shen, T. Zhuo, and H. Zhou, "Brain tumor segmentation based on refined fully convolutional neural networks with a hierarchical dice loss," *arXiv preprint arXiv:1712.09093*, 2017.
- [8] C. F. Baumgartner, L. M. Koch, M. Pollefeys, and E. Konukoglu, "An exploration of 2D and 3D deep learning techniques for cardiac MR image segmentation," in *International Workshop on Statistical Atlases and Computational Models of the Heart*, 2017, pp. 111-119: Springer.
- [9] Ö. Çiçek, A. Abdulkadir, S. S. Lienkamp, T. Brox, and O. Ronneberger, "3D U-Net: learning dense volumetric segmentation from sparse annotation," in *International conference on medical image computing and computer-assisted intervention*, 2016, pp. 424-432: Springer.
- [10] Z. Tian, L. Liu, and B. Fei, "Deep convolutional neural network for prostate MR segmentation," in *Medical Imaging 2017: Image-Guided Procedures, Robotic Interventions, and Modeling*, 2017, vol. 10135, p. 101351L: International Society for Optics and Photonics.
- [11] C. P. Ferdinand and E. F. MEE, "Automatic liver and lesions segmentation using Cascaded Fully Convolutional Neural Networks and 3D Conditional Random Fields," *MICCAI, p. PS4-18*, 2016.
- [12] X. Zhou *et al.*, "EAST: an efficient and accurate scene text detector," in *Proceedings of the IEEE conference on Computer Vision and Pattern Recognition*, 2017, pp. 5551-5560.
- [13] S. R. Buló, G. Neuhold, and P. Kontschieder, "Loss max-pooling for semantic image segmentation," in *2017 IEEE Conference on Computer Vision and Pattern Recognition (CVPR)*, 2017, pp. 7082-7091: IEEE.
- [14] O. Ronneberger, P. Fischer, and T. Brox, "U-net: Convolutional networks for biomedical image segmentation," in *International Conference on Medical image computing and computer-assisted intervention*, 2015, pp. 234-241: Springer.
- [15] S. A. Kamran and A. S. Sabbir, "Efficient yet deep convolutional neural networks for semantic segmentation," in *2018 International Symposium on Advanced Intelligent Informatics (SAIN)*, 2018, pp. 123-130: IEEE.
- [16] G. Litjens *et al.*, "Evaluation of prostate segmentation algorithms for MRI: the PROMISE12 challenge," *Medical image analysis*, vol. 18, no. 2, pp. 359-373, 2014.
- [17] M. Cordts *et al.*, "The cityscapes dataset for semantic urban scene understanding," in *Proceedings of the IEEE conference on computer vision and pattern recognition*, 2016, pp. 3213-3223.
- [18] D. P. Kingma and J. Ba, "Adam: A method for stochastic optimization," *arXiv preprint arXiv:1412.6980*, 2014.
- [19] D. E. Rumelhart, G. E. Hinton, and R. J. Williams, "Learning representations by back-propagating errors," *Cognitive modeling*, vol. 5, no. 3, p. 1, 1988.
- [20] M. Havaei *et al.*, "Brain tumor segmentation with deep neural networks," *Medical image analysis*, vol. 35, pp. 18-31, 2017.
- [21] M. Lai, "Deep learning for medical image segmentation," *arXiv preprint arXiv:1505.02000*, 2015.
- [22] M. Buda, A. Maki, and M. A. Mazurowski, "A systematic study of the class imbalance problem in convolutional neural networks," *Neural Networks*, vol. 106, pp. 249-259, 2018.
- [23] N. Jaccard, T. W. Rogers, E. J. Morton, and L. D. Griffin, "Detection of concealed cars in complex cargo X-ray imagery using deep learning," *Journal of X-ray Science and Technology*, vol. 25, no. 3, pp. 323-339, 2017.
- [24] G. Levi and T. Hassner, "Age and gender classification using convolutional neural networks," in *Proceedings of the IEEE conference on computer vision and pattern recognition workshops*, 2015, pp. 34-42.
- [25] G. Haixiang, L. Yijing, J. Shang, G. Mingyun, H. Yuanyue, and G. Bing, "Learning from class-imbalanced data: Review of methods and applications," *Expert Systems with Applications*, vol. 73, pp. 220-239, 2017.
- [26] N. V. Chawla, K. W. Bowyer, L. O. Hall, and W. P. Kegelmeyer, "SMOTE: synthetic minority over-sampling technique," *Journal of artificial intelligence research*, vol. 16, pp. 321-357, 2002.
- [27] K.-J. Wang, B. Makond, K.-H. Chen, and K.-M. Wang, "A hybrid classifier combining SMOTE with PSO to estimate 5-year survivability of breast cancer patients," *Applied Soft Computing*, vol. 20, pp. 15-24, 2014.
- [28] T. Jo and N. Japkowicz, "Class imbalances versus small disjuncts," *ACM Sigkdd Explorations Newsletter*, vol. 6, no. 1, pp. 40-49, 2004.
- [29] L. Shen, Z. Lin, and Q. Huang, "Relay backpropagation for effective learning of deep convolutional neural networks," in *European conference on computer vision*, 2016, pp. 467-482: Springer.
- [30] H. Guo and H. L. Viktor, "Learning from imbalanced data sets with boosting and data generation: the databoost-im approach," *ACM Sigkdd Explorations Newsletter*, vol. 6, no. 1, pp. 30-39, 2004.
- [31] C. Drummond and R. C. Holte, "C4. 5, class imbalance, and cost sensitivity: why under-sampling beats over-sampling," in *Workshop on learning from imbalanced datasets II*, 2003, vol. 11, pp. 1-8: Citeseer.
- [32] S. Lawrence, I. Burns, A. Back, A. C. Tsoi, and C. L. Giles, "Neural network classification and prior class probabilities," in *Neural networks: tricks of the trade*: Springer, 1998, pp. 299-313.
- [33] M. D. Richard and R. P. Lippmann, "Neural network classifiers estimate Bayesian a posteriori probabilities," *Neural computation*, vol. 3, no. 4, pp. 461-483, 1991.
- [34] M. Kukar and I. Kononenko, "Cost-Sensitive Learning with Neural Networks," in *ECAI*, 1998, pp. 445-449.
- [35] X. Li, L. Yu, D. Chang, Z. Ma, and J. Cao, "Dual cross-entropy loss for small-sample fine-grained vehicle classification," *IEEE Transactions on Vehicular Technology*, vol. 68, no. 5, pp. 4204-4212, 2019.
- [36] S. Iqbal, M. U. Ghani, T. Saba, and A. Rehman, "Brain tumor segmentation in multi - spectral MRI using convolutional neural networks (CNN)," *Microscopy research and technique*, vol. 81, no. 4, pp. 419-427, 2018.
- [37] S. Kullback and R. A. Leibler, "On information and sufficiency," *The annals of mathematical statistics*, vol. 22, no. 1, pp. 79-86, 1951.
- [38] K. He, X. Zhang, S. Ren, and J. Sun, "Deep residual learning for image recognition," in *Proceedings of the IEEE conference on computer vision and pattern recognition*, 2016, pp. 770-778.
- [39] M. Everingham, S. A. Eslami, L. Van Gool, C. K. Williams, J. Winn, and A. Zisserman, "The pascal visual object classes challenge: A retrospective," *International journal of computer vision*, vol. 111, no. 1, pp. 98-136, 2015.
- [40] T.-Y. Lin *et al.*, "Microsoft coco: Common objects in context," in *European conference on computer vision*, 2014, pp. 740-755: Springer.